Strong Selective Pressure To Use G:U To Mark an RNA Acceptor Stem for Alanine†

Joseph W. Chihade,‡,§ Kathleen Hayashibara,‡,|| Kiyotaka Shiba,⊥ and Paul Schimmel*,‡,§

Department of Biology, Massachusetts Institute of Technology, Cambridge, Massachusetts 02139, The Skaggs Institute for Chemical Biology, The Scripps Research Institute, 10550 North Torrey Pines Road, La Jolla, California 92037, and Department of Cell Biology, Cancer Institute, Japanese Foundation for Cancer Research, Kami-Ikebukuro, Toshima-ku, Tokyo 170-8455, Japan

Received February 26, 1998; Revised Manuscript Received April 24, 1998

ABSTRACT: The identity of alanine tRNAs is dependent on a G:U base pair at the 3:70 position of the acceptor helix. This system of molecular recognition is widely distributed from bacteria to human-cell cytoplasm. In contrast, some mitochondrial alanine acceptor helices are markedly different and contain nucleotides known to block aminoacylation by a nonmitochondrial enzyme. Thus, acceptor helix recognition may differ in these systems and may not depend on G:U. Here we report an example of a *Caenorhabditis elegans* mitochondrial system where the G:U pair is preserved but where proximal nucleotides known to block charging by a nonmitochondrial enzyme are also present. We show that, as expected, the mitochondrial substrate is not charged by the bacterial enzyme. In contrast, the cloned mitochondrial enzyme charged both mitochondrial and bacterial microhelices. Strikingly, charging of each required the G:U pair. Thus, G:U recognition persists even with an acceptor helix context that inactivates nonmitochondrial systems. The results suggest strong selective pressure to use G:U in a variety of contexts to mark an acceptor stem for alanine. Separate experiments also demonstrate that, at least for the mitochondrial enzyme, helix instability or irregularity is not important for recognition of G:U.

The universal genetic code is established in a single biochemical reaction—the aminoacylation of transfer RNAs. In this reaction, catalyzed by aminoacyl tRNA synthetases, amino acids are matched with anticodon nucleotide triplets in the tRNAs. To achieve specific aminoacylation, synthetases recognize information within the tRNA structure, and in some cases, that information does not include the anticodon triplet (*1*−*4*). In these instances, the relationship between the amino acid and its nucleotide triplets is indirect. In other examples, the anticodon is important for aminoacylation efficiency and specificity, but tRNA molecules with large deletions that remove the anticodon are still active for specific aminoacylation (*5*−*11*). In all of these examples—whether the synthetase does or does not contact the anticodon—critical elements that determine aminoacylation efficiency and specificity are located in the tRNA acceptor stem. This stem is thought to be a critical part of the earliest form of the tRNA structure (*12*, *13*). The relationship between the sequences/structure of acceptor stem oligonucleotides and the attached amino acid constitutes an operational RNA code for amino acids that may have preceded the genetic code (*14*).

Alanyl-tRNA synthetase is an example of a synthetase where no contact is made with the anticodon and where acceptor stem interactions have been preserved in widely distributed species, ranging from *Escherichia coli* to human cytoplasm (*2*, *15*−*17*). The acceptor stem of alanine and other tRNAs is comprised of seven base pairs that end in the single-stranded sequence $N^{73}CCA^{3'OH}$, where the 3′-terminal A contains the amino acid attachment site. Position 73 [in the standard tRNA nucleotide numbering system that is based on 76 nucleotides (*18*)] contains the discriminator base which was proposed to be a recognition site used by synthetases to sort tRNAs into four groups (*19*). In many instances, N^{73} has been found to be one of the critical determinants of the operational RNA code (*20*−*22*).

The three terminal bases pairs of the acceptor stem (G1:C72, G2:C71, and G3:U70) and the A73 "discriminator" base are conserved in all known $tRNA^{Ala}$ sequences from prokaryotes, archae, eukaryote cytoplasm, chloroplasts, and plant mitochondria (*23*). Two highly conserved elements that are critical for aminoacylation are a G3:U70 base pair and the A73 discriminator nucleotide. Alanine acceptance is conferred on other tRNA or minimalist RNA sequences by introducing a G3:U70 base pair (*2*, *24*−*26*). The exocyclic 2-amino group of G3 (in the G3:U70 base pair) is the major determinant (*27*, *28*). Other, proximal atomic groups, including specific 2′-OH groups are also important for charging efficiency (*29*−*32*). This acceptor stem sequence is sufficient for charging of minimal RNA substrates with as few as four base pairs (*26*).

Conservation through evolution is also evident on the protein side of the interaction. Alanyl-tRNA synthetase is the most conserved of the 20 aminoacyl-tRNA synthetases (*16*). The enzymes exhibit a linear organization of functional domains (*33*, *34*) in which an N-terminal core domain (about

† This work was supported by National Institutes of Health Grants GM15539 and GM23562. J.W.C. and K.H. were supported by NIH postdoctoral fellowships.

* To whom correspondence should be addressed.
‡ Massachusetts Institute of Technology.
§ The Scripps Research Institute.
⊥ Japanese Foundation for Cancer Research.
|| Present address: Department of Biochemistry, Stanford University School of Medicine, Stanford, CA 94304.

S0006-2960(98)00463-2 CCC: $15.00
Published on Web 06/05/1998

one-half of the protein structure) is made up of the class II active site domain and an RNA recognition domain. This core domain is sufficient for aminoacylation in the *E. coli* system (*33*, *35*, *36*). The core domain is highly conserved, with 41% identity between the *E. coli* and human enzymes (*16*).

The functional conservation of AlaRS-acceptor stem recognition is demonstrated by the several examples of cross-species recognition. *E. coli* AlaRS charges small RNA substrates based on acceptor stems of alanine tRNAs from *Saccharomyces cerevisiae*, *Bombyx mori*, and human cytoplasm (*17*, *37*). More significantly, cross-species reactivity has also been demonstrated *in vivo*. For example, expression of the human alanine enzyme rescues a knockout allele of *S. cerevisiae* AlaRS (*17*).

Remarkably, conservation of the $tRNA^{Ala}$ acceptor stem terminus is not observed in sequences from animal mitochondria. Every animal mitochondrial $tRNA^{Ala}$ thus far identified contains at least one sequence variation in the first three base pairs from the conserved prokaryote/eukaryote cytoplasm sequence noted above (*23*). Each of the sequences, however, also contains at least one of the elements of the conserved prokaryote/eukaryote cytoplasm pattern. Some of these mitochondrial tRNAs also diverge from the canonical cloverleaf structure, differing in the lengths of stems and the sizes of loops (*38*). Among the most unusual mitochondrial tRNAs are those from the nematode worm *Caenorhabditis elegans*. All mitochondrial tRNAs from this organism lack either the D- or T-stem-loop (*39*, *40*). These unusual RNAs can be folded into a truncated L-shaped, tRNA-like structure (*41*, *42*).

The sequence of *C. elegans* mitochondrial $tRNA^{Ala}$ is compared with that from *E. coli* in Figure 1. This 3/4 molecule completely lacks the TΨC stem-loop and variable loops, which are replaced by a six nucleotide connector between the anticodon and acceptor stem sequences. The D-loop is shortened, consisting of only five nucleotides, as opposed to eight in the canonical tRNA secondary structure (*18*). The mitochondrial tRNA is also A:U-rich, with only two G:C base pairs in the entire secondary structure.

The *C. elegans* mitochondrial $tRNA^{Ala}$ differs from the consensus alanine acceptor stem sequence in that the acceptor helix ends in a G1:U72 wobble pair, compared with the consensus G:C pair. However, the presence of a G1:U72 base pair blocks charging by *E. coli* alanyl-tRNA synthetase (AlaRS) (*32*). Using base analogue substitutions at the 1:72 position, the 4-position carbonyl oxygen of the pyrimidine ring of U72 was identified as a blocking element (for the *E. coli* enzyme) on the major groove side of the helix.

The examination of the *C. elegans* mitochondrial alanyl-tRNA synthetase thus presents an opportunity to investigate the recognition of specific identity elements in a different RNA context and to explore the coadaptations in evolution of the alanine enzymes to accommodate changes in sequence and structure of their substrates. The *C. elegans* mitochondrial alanyl-tRNA synthetase must charge a substrate which the *E. coli* [and presumably a large group of closely related alanyl-tRNA synthetases (see above)] cannot acylate. The enzyme must either recognize conserved identity elements in a different RNA context than its homologues, or utilize an entirely different set of RNA contacts to identify its substrate. With these considerations in mind, we cloned and

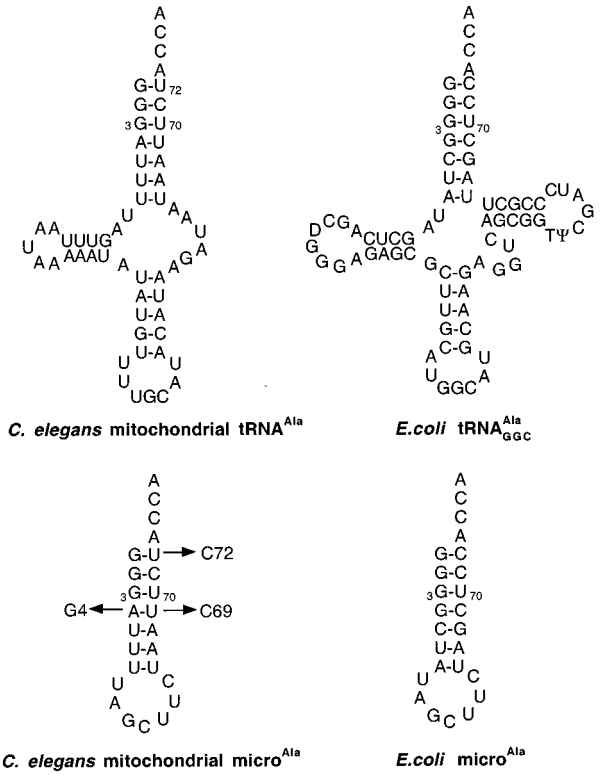

FIGURE 1: *C. elegans* mitochondrial and *E. coli* $tRNA^{Ala}$ (*23*). Microhelix substrates based on the acceptor stems of the tRNAs are also shown. Mutations of *C. elgans* mitochondrial $microhelix^{Ala}$ discussed in the text are indicated with arrows.

expressed *C. elegans* mitochondrial alanyl-tRNA synthetase and investigated microhelix oligonucleotides as substrates for aminoacylation. The results revealed that the *C. elegans* mitochondrial enzyme is a close homologue of other alanine enzymes, including the well-characterized *E. coli* protein. The enzyme is active on microhelix substrates, like its *E. coli*, yeast, *B. mori*, and human counterparts. And yet, the mitochondrial *C. elegans* enzyme charges a microhelix substrate (based on the acceptor stem of mitochondrial *C. elegans* $tRNA^{Ala}$) that is not charged by the *E. coli* enzyme. This result raised the possibility that the mitochondrial enzyme was fundamentally different and did not utilize, for example, the G3:U70 base pair. Subsequent experiments disproved this possibility and, instead, demonstrated a remarkable selective pressure for the mitochondrial *C. elegans* alanyl-tRNA synthetase structural framework to maintain G3:U70 recognition in the context of acceptor stem sequences that block G3:U70-dependent aminoacylation by its close homologue.

MATERIALS AND METHODS

Cloning of C. elegans Alanyl-tRNA Synthetases by an Alignment-Guided Approach. A similar approach to that used for cloning human cytoplasmic alanyl-tRNA synthetase (*16*) was applied to cloning the *C. elegans* alanyl-tRNA synthetases. Degenerate primers were designed which correspond to two highly conserved regions of alanyl-tRNA synthetases within the active-site domain, starting at codons 38 and 86, respectively, of the *E. coli* enzyme. These primers were KY-23 (TTYRCIAAYGCIGGIATGAAYCARTTY-AAR) and KY-25 (RTTICCCATCATYTCRAARAAIGTRT-GRTG), where Y is pyrimidine, R is purine, and I is inosine.

The primers were used for PCR amplification of the desired sequences from a *C. elegans* cDNA library that was cloned into the λZAPII phagemid (*43*). Amplified products were ligated to *Bam*HI linkers and cloned into the *Bam*HI site of pBluescript II KS+ (Stratagene, La Jolla, California) for sequencing. Two distinct sequences were identified from the sequencing of nine clones. These sequences could be translated into amino acid sequences that bore similarity to known sequences for alanine tRNA synthetases. Internal primers based on these sequences were subsequently used, along with primers based on sequences within the vector, to amplify 5′- and 3′-ends of each cDNA. The two cDNA sequences were obtained that contained open reading frames encoding polypeptides with 272 and 792 amino acids that we denoted AlaRS A and AlaRS B, respectively.

Expression and Purification of AlaRS B. To simplify purification of expressed protein, the AlaRS B sequence was subcloned into the expression vector pET21b (Stratagene, La Jolla, California), which utilizes a T7 promoter and introduces a His_6 sequence at the C-terminal end of the cloned polypeptide coding sequence. PCR was used to introduce appropriate restriction sites at the 5′- and 3′-termini of the AlaRS B cDNA. For this purpose, primers TAGGGC-*CATATG*GGAATTGGCTCCA and TCTAGG*CTCGAG*TTT-CTTCTGTTTCAGC (restriction sites in italics) were used to amplify the AlaRS B sequence, introducing *Nde*I and *Xho*I sites, respectively, at the 5′- and 3′-ends. Subcloning of this PCR product into plasmid pET21b resulted in the extension of the C-terminal end of the cDNA with the peptide coding sequence LEHHHHHH.

Because products of proteolysis were observed in attempts to express full-length AlaRS B, an expression vector which excluded the N-terminal 17 amino acids was designed. This N-terminal sequence precedes the beginning of the region of sequence similarity with alanyl-tRNA synthetases from other organisms and thus was presumed to be a mitochondrial targeting sequence. To minimize the possibility of carrying over errors introduced by previous PCR manipulations, a unique cDNA clone encoding the AlaRS B sequence was used as a template for PCR. EST yk43h10, generated as part of the *C. elegans* genome project, was a gift from Dr.Yuji Kohara (National Institute of Genetics, Mishima, Japan). The 5′- and 3′-sequences of this cDNA clone showed that the clone contains the entire AlaRS B sequence obtained by us. The sequence was amplified by PCR from phage containing the EST yk43h10, using the primer GCGCGC-CATATGGGATTCTATCATTCAC and the primer described above for the 3′-terminus of AlaRS B cDNA. The resulting PCR product again contained *Nde*I and *Xho*I restriction sites at the 5′- and 3′-termini, with Gly19 of the protein sequence encoded directly after the ATG start codon that was included in the *Nde*I site. The amplified product was subcloned into the pET21b expression vector to give plasmid pD18−43h. This plasmid was transformed into *E. coli* strain BL21(DE3) (*44*) for expression.

Cells were grown in LB medium supplemented with 50 μg/mL ampicillin to OD_{600} of 0.6 and then inoculated with IPTG to a final concentration of 0.4 mM. The cells were grown an additional 4 h and then harvested and lysed in a French press. The His_6-tagged enzyme was purified on a Ni−NTA agarose (Qiagen, Santa Clarita, California) column in 50 mM Na_2HPO_4 (pH 8.0), 300 mM NaCl, and 10% glycerol. Elution was with a gradient of 20−100 mM imidazole. Mitochondrial AlaRS obtained in this manner was ∼90% pure, with major contaminants being apparent degradation products. In the case of the *E. coli* protein, The His_6-tagged enzyme was isolated as previously described (*45*). The AlaRS A enzyme was not pursued further for reasons described below.

Determination of Quaternary Structure of C. elegans Mitochondrial Alanyl-tRNA Synthetase. The quaternary structure of the expressed *C. elegans* AlaRS B enzyme under native conditions was determined using Superose 12 gel filtration chromatography. A Superose 12 10/30 column (Pharmacia, Piscataway, NJ) was equilibrated with 50 mM Na_2HPO_4 (pH 8.0), and 10% glycerol. All samples were applied in 50 μL. A standard curve was constructed by separate elution of ferritin (669 kDa), catalase (232 kDa), aldolase (158 kDa), and serum albumin (67 kDa). Elution positions of standard proteins and of *C. elegans* mitochondrial alanyl-tRNA synthetase were determined by optical density at 280 nM.

RNA Substrates and Aminoacylation Assays. Microhelix RNA substrates were chemically synthesized on a Pharmacia Gene Assembler synthesizer using published procedures (*46*). Products of the syntheses were purified on denaturing 20% polyacrylamide gels. Melting curves were constructed from absorbance data obtained using a Cary 3E spectrophotometer equipped with a temperature controller. Oligonucleotides were annealed in 10 mM Na_2HPO_4 (pH 7.0), 10 mM NaCl, and 0.1 mM EDTA. Absorbances were measured over a range from 10 to 85 °C at a rate of 2 °C/minute with a data interval of 1 °C.

Aminoacylation assays were carried out at 25 °C in 50 mM Hepes (pH 7.5), 20 μM alanine, 4 mM ATP, 20 mM KCl, 10 mM $MgCl_2$, 20 mM β-mercaptoethanol, and 0.1 mg/mL bovine serum albumin, as previously described (*47*). To ensure proper base pairing, microhelices were heated to 65 °C and cooled in the absence of magnesium before addition to the aminoacylation reaction mixture. In comparative assays, RNA was at a concentration of 4.5 μM, while enzyme concentrations were 45 nM. [All enzyme concentrations were determined by active site titration (*48*).] Kinetic parameters for *C. elegans* mitochondrial AlaRS and *E. coli* AlaRS were determined by direct fitting of data points to the Michaelis−Menten equation. Initial rates were determined at 25 °C with RNA concentrations from 20 to 400 nM for the *C. elegans* mitochondrial microhelix and from 13 to 64 μM for the *E. coli* microhelix. Enzyme concentrations of 15 nM were used in both cases.

RESULTS

Cloning of C. elegans Alanyl-tRNA Synthetases. Aminoacyl tRNA synthetases are divided into two classes of 10 enzymes each (*49, 50*). These classes are based on the particular architecture of the active-site domain. Alanyl-tRNA synthetase is a class II enzyme. Members of class II have an active-site domain comprised of a seven stranded β-structure with three α-helices. This class-defining structure incorporates three highly degenerate sequence motifs that are characteristic of the class II enzymes. These motifs are designated as motifs 1, 2, and 3, and comprise a strand-loop-helix, strand-loop-strand, and strand-helix, respectively.

To clone the *C. elegans* enzymes, we used an approach similar to that used for cloning human cytoplasmic alanyl-tRNA synthetase (*16*). Degenerate primers were designed to correspond to well-conserved regions of the enzyme. Sequence alignment of 18 complete and partial alanyl-tRNA synthetase sequences showed that sequences in motif 1 and motif 2 are among the most conserved regions in the enzyme. We therefore used the same degenerate primers to clone the cDNAs for the *C. elegans* synthetases as were used for the cDNA of the human enzyme.

The PCR products that were amplified from a *C. elegans* cDNA library were cloned into pBluescript II KS+ and sequenced. Two distinct sequences of less than 200 base pairs were identified. These were used to design primers for the amplification of 5′- and 3′-sequences from the cDNA. Full-length amplified products were then cloned and sequenced. Two distinct AlaRS open reading frames were thus identified. AlaRS A encodes a 272 amino acid predicted polypeptide, while AlaRS B encodes a predicted protein of 792 amino acids.

While this work was in progress, portions of the *C. elegans* genome containing both of these sequences became available (*51*). These genomic sequences include both introns and exons. Coding sequences were predicted using the splice-site prediction algorithm Genefinder. AlaRS A corresponds to a fragment of a predicted coding sequence of 967 amino acids contained in Genbank locus CELF28H1, while AlaRS B is highly similar to a predicted coding sequence in Genbank CEW02B12. The predicted sequence of AlaRS B available in the database differs from the cDNA sequence reported here in that the predicted sequence fails to exclude a 331 nucleotide intron from position 1624 to 1954 of the genomic sequence. Analysis with a different splice site prediction program, FGENEN (*52*), which has parameters specifically for nematode genomes, predicted an expressed sequence matching that obtained from the cDNA for AlaRS B.

In prokaryotes, there is most commonly only one synthetase for each amino acid. In the case of eukaryotes, there typically are two enzymes for each amino acid—a cytoplasmic and a mitochondrial synthetase, both of which are nuclear encoded. Therefore, we imagined that the two sequences we obtained corresponded to a cytoplasmic and mitochondrial form of alanyl-tRNA synthetase. By having cloned and sequenced part or all of both instead of one enzyme, we were able to make an assignment (mitochondrial or cytoplasmic) for each, without fear that a missing sequence could change our conclusions.

Assignment of AlaRS B as the mitochondrial synthetase was made on the basis of three criteria. First, sequence alignment of the 792 amino acid AlaRS B product with known sequences of alanyl-tRNA synthetases revealed an N-terminal extension of between 12 and 18 amino acids in the sequence of AlaRS B (Figure 2). This extension was not present in the 967 amino acid sequence predicted for AlaRS A. Nuclear-encoded mitochondrial proteins generally have an N-terminal targeting peptide, which directs their translocation to the mitochondria (*53*). These peptides usually lack acidic amino acids and are rich in positively charged and hydroxyl group side chains. Many of these peptides fold into amphiphilic α-helical or β-sheet structures. Although the N-terminal sequence of AlaRS B contains a glutamate residue at position 8, it otherwise follows the pattern of a mitochondrial protein. For example, five of the first 16 residues are either serine or lysine, and residues 7−17 are predicted to form an amphiphilic α-helix.

Second, assignment of AlaRS B as a mitochondrial enzyme was supported by an additional signature in its sequence. In particular, eukaryote cytoplasmic alanyl-tRNA synthetases contain a four residue insert immediately prior to motif 2 of the active-site domain (between residues 58 and 59 of the *E. coli* enzyme's sequence). While the predicted AlaRS A sequence contains this insert, the AlaRS B sequence does not, and in this aspect, AlaRS B is prokaryote-like, as are many mitochondrial enzymes.

Third, phylogenetic analysis utilizing parsimony methods and bootstrapping (*54*) (Figure 3) showed that AlaRS A groups with *B. mori* and human cytoplasmic alanyl-tRNA synthetases, while AlaRS B does not group strongly with either eukaryote or prokaryote enzymes. Comparison of sequence identities of the two *C. elegans* proteins with known alanyl-tRNA synthetases underscored this result. AlaRS A has 55% identity with human cytoplasmic AlaRS, but only 36% identity with the *E. coli* enzyme. On the other hand, AlaRS B has comparable identities of 31 and 27% with the human and *E. coli* enzymes, respectively. Thus, sequence comparisons and phylogenetic analysis are most consistent with the conclusion that AlaRS B encodes the mitochondrial synthetase, while AlaRS A encodes the cytoplasmic protein.

Expression of C. elegans Mitochondrial alanyl-tRNA Synthetase in E. coli. To expedite purification of the mitochondrial enzyme, an expression system based on the T7 RNA polymerase promoter was constructed. A His_6-coding sequence was appended to the C-terminus of the protein sequence. [Attachment of a His_6-tag to the C-terminus of the *E. coli* protein does not interfere with activity (*45*).] Initial attempts to express full-length AlaRS B in *E. coli* using this system yielded overexpression of a polypeptide with a molecular mass of ∼48 kDa, as judged by SDS−PAGE. This peptide is presumably the product of proteolysis of the full-length AlaRS B.

Because mitochondrial targeting peptides are generally removed by proteolysis from nuclear-encoded mitochondrial proteins after translocation to the organelle (*53*), we hypothesized that the targeting peptide may act as a proteolysis signal in the *E. coli* cytoplasm. Thus, an expression system was generated (by PCR) in which the N-terminal 18 amino acids of the His-tagged AlaRS B were removed. (Sequence similarity between the *E. coli* enzyme and AlaRS B begins at Gly19 of the *C. elegans* sequence.) Using this system, expression of full-length protein was obtained, though at relatively low levels. The expressed protein was isolated to ∼90% purity by affinity chromatography on Ni−NTA agarose. Proteolytic products were the major contaminants, suggesting that removal of the N-terminal sequence results in only a partial stabilization of the mitochondrial protein in an *E. coli* background. Western blot analysis (with anti-*E. coli* AlaRS antibodies) of the purified mitochondrial protein resolved by SDS−PAGE revealed no detectable contamination with *E. coli* AlaRS (data not shown).

Determination of Quaternary Structure of C. elegans Mitochondrial Enzyme. One of the major differences between alanyl-tRNA synthetases in prokaryotes and eukaryotes is in their quaternary structures. Prokaryote en-

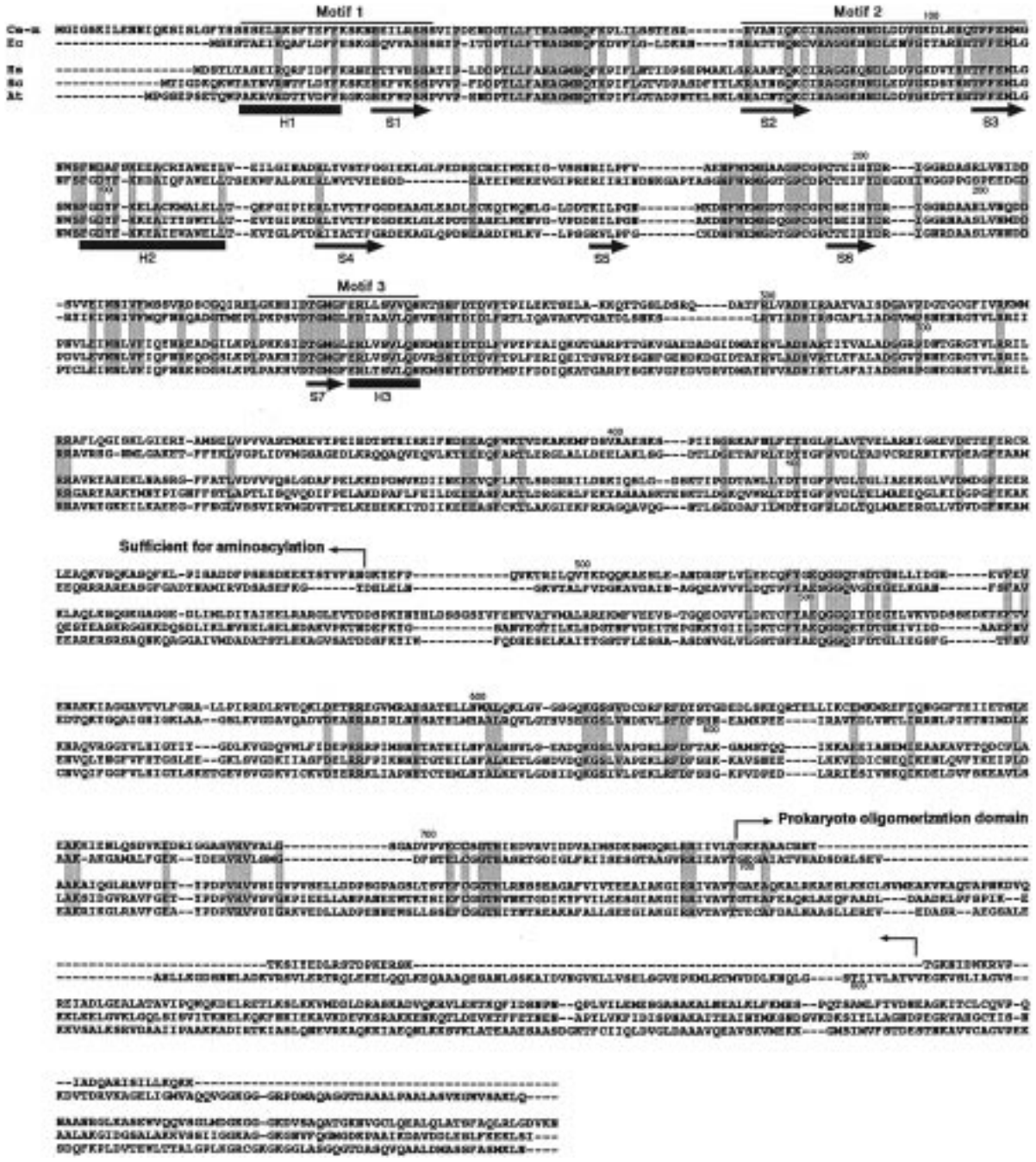

FIGURE 2: Multiple sequence alignment of alanyl-tRNA synthetases. The CLUSTAL-W program was used to align alanyl-tRNA synthetases from *E. coli* (Ec), *Homo sapiens* (Hs), *S. cerevisae* (Sc), *A. thaliana* (At), and *C. elegans* mitochondria (Ce-m). Residues conserved among the five sequences are shaded. Numbering at top corresponds to the *C. elegans* mitochondrial enzyme, at bottom to the *E. coli* sequence. Predicted secondary structure elements in the core region of the *E. coli* enzyme are indicated by bars (α-helices) and arrows (*β*-strands) (*45*). The functional core region of the *E. coli* enzyme is indicated, and the location of the oligomerization region found in the prokaryote enzymes is also shown.

zymes are in general α_4 tetramers, while those from eukaryotes are monomers. The quaternary structure of the expressed *C. elegans* enzyme under native conditions was determined by gel filtration chromatography on Superose 12. Ferritin (669 kDa), catalase (232 kDa), aldolase (158 kDa), and serum albumin (67 kDa) were used as standards. An empirical molecular mass of 85.8 kDa was determined for AlaRS B (data not shown). This molecular mass compares well with the value of 87.7 kDa that is predicted from the sequence. These data show that the *C. elegans* mitochondrial enzyme is a monomer.

Prokaryote alanyl-tRNA synthetases contain a C-terminal domain which forms a coiled-coil that is needed for formation of a tetrameric structure (*33*, *55*−*57*). Removal of this domain from the *E. coli* enzyme results in a functional monomer (*33*, *56*, *58*). In the eukaryote alanyl-tRNA synthetases, the sequences of the C-terminal region corresponding to the coiled-coil found in the prokaryote enzymes are completely different (*16*). This difference in sequence correlates with these eukaryote enzymes being monomeric. *C. elegans* mitochondrial alanyl-tRNA synthetase is roughly 100 amino acids shorter than available prokaryote or cytoplasmic

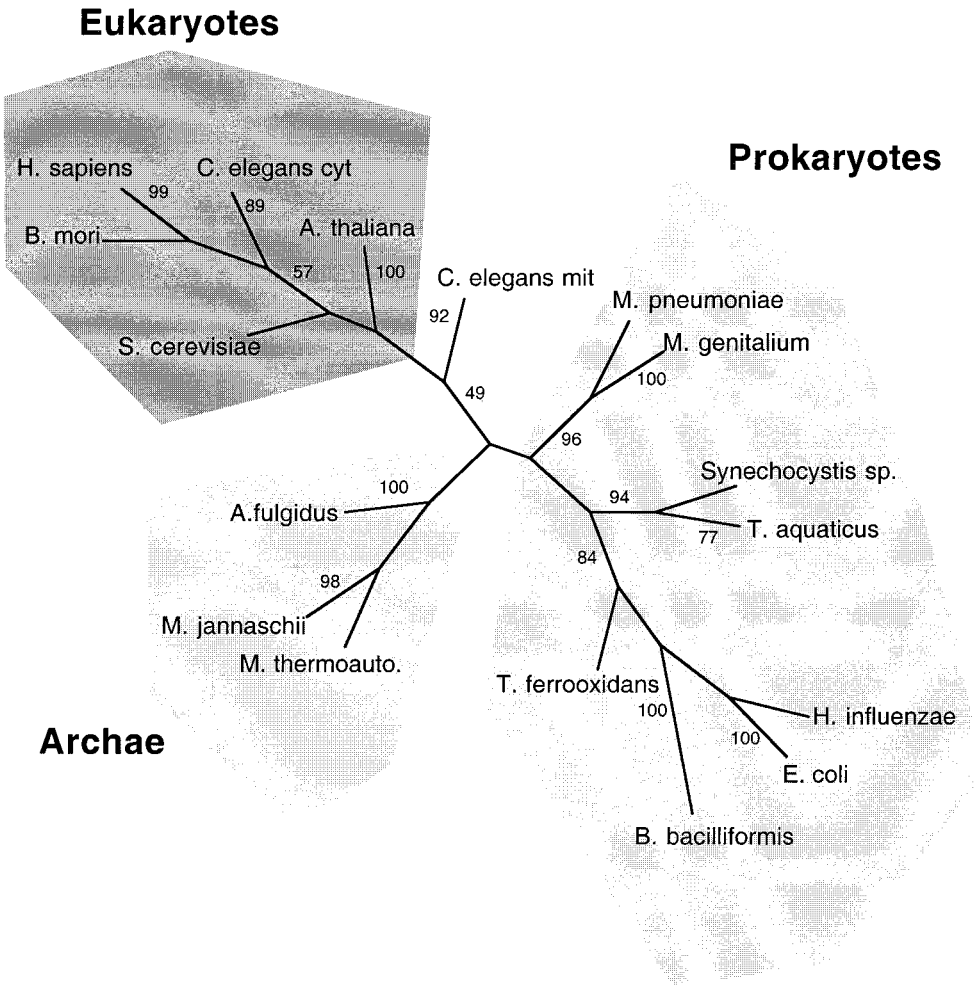

FIGURE 3: Evolutionary relationship of alanyl-tRNA synthetase sequences. Unrooted tree prepared using the parsimony method [PROTPARS from the PHYLIP phylogeny package (*55*)] with bootstrapping. Numbers at branches are bootstrap percentages with 100 replicates.

eukaryote alanine enzyme sequences, and it lacks sequence similarity with either set of enzymes in the C-terminal region (Figure 2).

Many class II tRNA synthetases are dimers; dimerization is facilitated through an interface that includes the region of the conserved motif 1. In the case of *E. coli* AlaRS, motif 1 cooperates with the C-terminal coiled-coil domain to create the tetrameric quaternary structure (*57*). For the alanine enzymes, a clear delineation of prokaryote multimers and eukaryote monomers coincides with the identity of a single amino acid in motif 1. An aspartate is found in position 48 (using the sequence of *E. coli* AlaRS for numbering) in the prokaryotes, while in eukaryotes this position is a proline. In the case of the *C. elegans* mitochondrial AlaRS investigated here, a proline is found at this position (Figure 2), consistent with the enzyme's observed monomeric structure.

Mitochondrial Enzyme Aminoacylates RNA Substrates Based on Acceptor Stems of Alanine tRNA from C. elegans Mitochondria or E. coli. In these studies, we focused on acceptor helix interactions and for that reason used microhelix RNA substrates. We prepared (by chemical synthesis) microhelix substrates that reconstructed the seven base pair acceptor stem of *C. elegans* mitochondrial $tRNA^{Ala}$. Because the mitochondrial microhelix contains three mismatched base pairs [G1:U72, G3:U70, and U7:U66 (Figure 1)], we were concerned that the oligonucleotide would not form the desired hairpin structure in aminoacylation assays. A melting temperature of 35 °C was determined for the mitochondrial microhelix substrate, as compared to a T_m of 72 °C for a microhelix based on the acceptor stem of *E. coli* $tRNA^{Ala}$ (data not shown). (These melting temperatures were not concentration dependent.) All aminoacylation assays were therefore carried out at 25 °C to ensure proper helix formation by the RNA substrates.

All alanyl-tRNA synthetases tested to date are active on microhelix substrates, but none of these substrates have the G1:U72 base pair that is detrimental to the *E. coli* and probably other alanine enzymes. However, the *C. elegans* mitochondrial $microhelix^{Ala}$ was charged by the mitochondrial enzyme (Figure 4). The value of k_{cat}/K_m (3.5×10^5 M^{-1} s^{-1}) is about 30-fold higher than that of the *E. coli* enzyme on its substrate, under the same experimental conditions of pH 7.5, 25 °C (data not shown).

We also tested a microhelix based on the acceptor stem of *E. coli* $tRNA^{Ala}$, which differs at the important 1:72 position and also at the 4:69, 5:68, and 7:66 positions (Figure 1). This microhelix was also efficiently charged by the mitochondrial enzyme, with about the same efficiency as that directed toward the *C. elegans* $microhelix^{Ala}$ substrate.

Finally, the same two substrates were tested with the *E. coli* enzyme. We were interested to see whether the lower helix stability and substitutions at the 4:69, 4:68, and 7:66 positions of the *C. elegans* $microhelix^{Ala}$ could compensate for the deleterious G1:U72 base pair. [Musier-Forsyth and

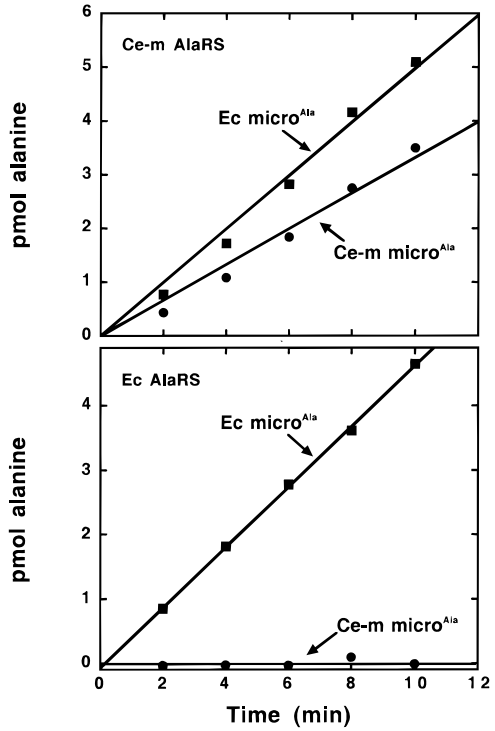

FIGURE 4: (a) Aminoacylation of microhelices by *C. elegans* mitochondrial AlaRS. (b) Aminoacylation of microhelices by *E. coli* AlaRS.

co-workers (*59*) showed that a C72U replacement results in a 4100-fold decrease in aminoacylation efficiency of tRNA^{Ala} transcripts. Because most *E. coli* tRNAs have a G1:C72 base pair, this base pair does not serve a role in differentiating between tRNAs but rather establishes a particular context and structure for the other portions of the acceptor stem.] However, the *E. coli* enzyme is inactive on mitochondrial microhelix^{Ala}, probably because the unique sequence context of *C. elegans* microhelix^{Ala} does not compensate for the G1:U72 base pair.

Thus, recognition by the *C. elegans* mitochondrial enzyme differs in a fundamental way from that of the *E. coli* protein. This difference raised our interest in the question of whether the G3:U70 base pair was critical for the mitochondrial protein as it is for other prokaryote and eukaryote cytoplasmic alanyl-tRNA synthetases.

G3:U70 Base Pair Is a Determinant for Charging by C. elegans Mitochondrial AlaRS. For *E. coli* alanyl-tRNA synthetase, replacement of U70 with C in alanine-accepting substrates results in a drop in aminoacylation efficiency by several-hundred- to several-thousand-fold, depending on the RNA context (*60*). Substrates with substitutions at 3:70, such as A:U, U:G, and I:U among others, are also inactive for *in vitro* aminoacylation. In the present studies, we found that a C70 substitution into *C. elegans* mitochondrial microhelix^{Ala} caused a sharp drop in charging by the *C. elegans* mitochondrial enzyme (about 40-fold reduced, Figure 5). Although this aminoacylation rate difference between G3:U70 and G3:C70 substrates is less dramatic than that observed for *E. coli* AlaRS, the G3:U70 pair nonetheless significantly determines recognition by the mitochondrial synthetase. Therefore, while the mitochondrial enzyme is not sensitive to the nature of the 1:72 base pair and can accommodate at this position base pair variants that block

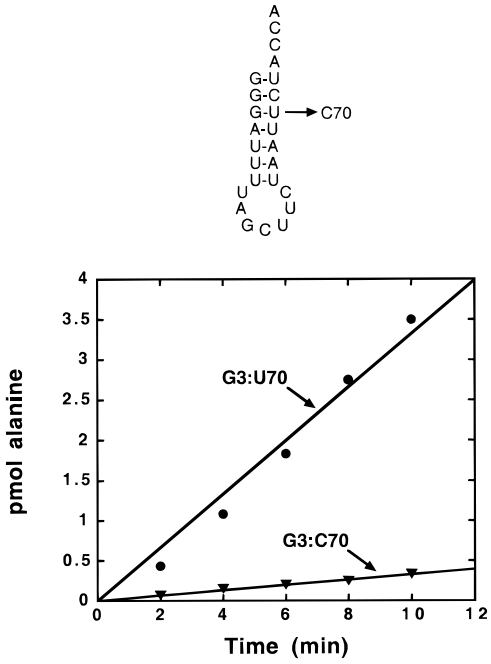

FIGURE 5: Importance of the G3:U70 base pair. Aminoacylation of *C. elegans* mitochondrial microhelix^{Ala} containing a G3:U70 or G3:C70 base pair.

charging by the *E. coli* protein, selective pressure overrides these differences to maintain G3:U70 as critical for acceptor helix recognition.

Additional Functional Differences between the Two Alanyl-tRNA Synthetase Homologues. To characterize further the functional differences between the two alanyl-tRNA synthetase homologues, nucleotides from the *E. coli* tRNA^{Ala} acceptor stem were introduced into RNA microhelices that were based on the acceptor stem of the *C. elegans* mitochondrial tRNA^{Ala}. These substitutions were done in a stepwise manner. With respect to the *E. coli* enzyme, substitutions at the 1:72 and 4:69 positions were required to convert the *C. elegans* substrate into one that was equivalent to the *E. coli* microhelix^{Ala} (Figure 6). For example, no charging was detected for any of the substrates containing a U72 nucleotide, as was expected. When U72 in the mitochondrial sequence is replaced by C, the microhelix is charged at a rate within 4-fold of that observed for the *E. coli* sequence. The additional replacement of the A4:U69 with the G:C found in *E. coli* tRNA^{Ala} leads to charging at a rate comparable to that for the *E. coli* microhelix^{Ala}. However, this 4:69 change alone does not induce charging by *E. coli* AlaRS, because of the presence of the G1:U72 base pair.

Charging of microhelix substrates by *C. elegans* mitochondrial AlaRS is completely unaffected by the change at position 72 or at the 4:69 base pair (Figure 6). All of the mutant mitochondrial microhelices are charged at identical rates by the mitochondrial enzyme. Therefore, changes in the sequence and shape of the acceptor helix which have a significant effect on RNA recognition for *E. coli* alanyl-tRNA synthetase are of no relevance for the *C. elegans* mitochondrial synthetase. The insensitivity of the mitochondrial enzyme to the base pairs at the 1:72 and 4:69 positions further emphasizes the significance of the sensitivity of the enzyme to the presence of the G3:U70 base pair.

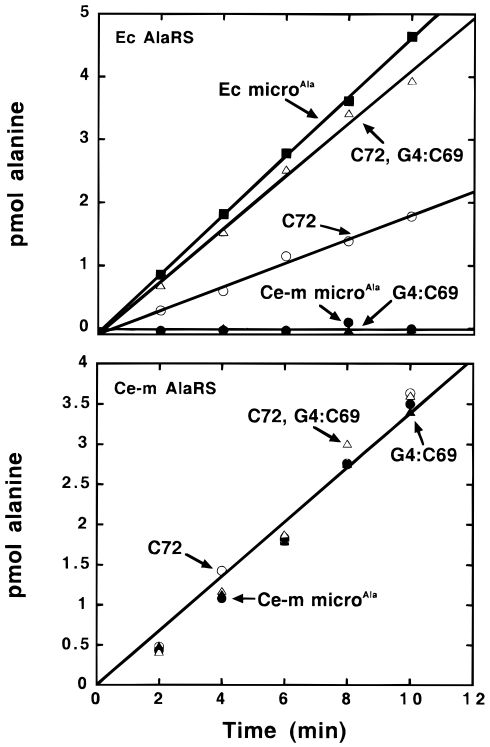

FIGURE 6: RNA determinants for microhelix aminoacylation. (a) Aminoacylation of microhelix RNAs by *E. coli* AlaRS. (b) Aminoacylation of microhelix RNAs by *C. elegans* mitochondrial AlaRS. The effects of nucleotide substitutions in the Ce-m microhelix are shown.

DISCUSSION

To examine the differences in RNA recognition which compensate for differences in acceptor stem sequences between alanine tRNAs from animal mitochondria and those from other sources, we set out to clone and express a mitochondrial alanyl-tRNA synthetase. The choice of *C. elegans* as the first target was attractive because of the difference in acceptor stem sequence (a G:U wobble pair in the 1:72 position) that prevents charging by a prokaryotic homologue and because of the possibility that the unique 3/4-molecule nature of mitochondrial tRNAs from nematode worms would manifest itself in a novel mitochondrial tRNA synthetase. The success of homology-based PCR for cloning the mitochondrial enzyme, as well as the overall sequence similarity (22−32% identity) to alanyl-tRNA synthetases cloned from a wide variety of organisms, showed that many features of AlaRS are conserved despite the changes in the RNA substrate.

We thought that the small size of the mitochondrial enzyme (774 amino acids if the mitochondrial targeting peptide is removed) relative to AlaRS sequences from prokaryotes and eukaryote cell cytoplasm (874−968 amino acids) might correlate with the reduced size of its 3/4-tRNA substrate. The N-terminal half of the alanyl-tRNA synthetases consists of the class-defining active-site domain followed by domains which have been implicated in acceptor stem sequence recognition. Truncation of the *E. coli* AlaRS after these domains results in a decrease in charging efficiency for full-length tRNA but has no effect on charging of mini- or microhelix substrates (*61*). These data suggested that the C-terminal half of the enzyme interacted with portions of the tRNA other than the acceptor helix. The details of these interactions have yet to be determined. However, the mitochondrial enzyme's sequence is similar to both prokaryote and eukaryote AlaRS sequences in the N-terminal core domain (Figure 2). Although "missing" portions outside of the N-terminal core might be thought to be those involved in interactions with parts of the tRNA structure outside of the acceptor stem, we have no evidence for this possibility. In particular, RNA footprint analysis of the complex between *E. coli* alanyl-tRNA synthetase and tRNA^{Ala} (*15*) showed that little of the region that is deleted from the mitochondrial tRNA^{Ala} makes contact with the bound enzyme.

The presence of a nucleotide (U72) known to block charging by *E. coli* alanyl-tRNA synthetase in the *C. elegans* mitochondrial tRNA sequence seemed initially to be analogous to the species-specific recognition exhibited by other synthetases. For example, glycyl-tRNA synthetases from *E. coli* and from human cytoplasm are unable to cross-acylate, respectively, human and *E. coli* tRNA^{Gly} (*62*). Switching a single nucleotide (the N73 discriminator base: A in humans and U in bacteria) in minihelix RNA substrates reversed the specificity of the enzymes (*22*).

Tyrosyl-tRNA synthetases provide another example of species-specific acceptor stem recognition. As in the glycine case, tyrosyl-tRNA synthetases from prokaryotes and eukaryotes cannot cross-acylate the respective tyrosine tRNAs (*10, 63*). The basis for this discrimination is the 1:72 base pair. In prokaryotes, a G:C pair common to most tRNAs is found in this position while, in eukaryotes, it is a C:G pair. Switching this single base pair is sufficient to switch substrate specificity of tyrosyl-tRNA synthetases both for full-length tRNA (*63*) and for microhelix RNA substrates (*10*). The 1:72 base pair appears to interact with an insertion that splits the active-site domains of class I synthetases, of which TyrRS is an example. A subpart of this insertion, which is comprised of just 39 amino acids, is sufficient to switch species-specific acylation. The switch was accomplished by transplanting the peptide from a human TyrRS into *E. coli* TyrRS and, reciprocally, by transplanting the analogous peptide from the *E. coli* synthetase into the human enzyme (*64*).

The differences in substrate recognition between *E. coli* and *C. elegans* mitochondrial alanyl-tRNA synthetases are distinct from the species-specific recognition described above in that the inability to cross-acylate substrates from a different species is not reciprocal. While *E. coli* AlaRS is unable to charge RNAs derived from the mitochondrial tRNA, the mitochondrial synthetase is able to charge both its own substrate and to cross-acylate a substrate based on the acceptor stem of *E. coli* tRNA^{Ala}. *E. coli* AlaRS fails to charge the *C. elegans* mitochondrial RNA because of the presence of a specific *negative* determinant. Charging is blocked by the presence in the major groove of the 4-keto oxygen of U72 (*32*). Adaptations which allow *C. elegans* mitochondrial AlaRS to charge the mitochondrial tRNA make the enzyme insensitive to the presence of the 4-keto oxygen that specifically blocks the *E. coli* enzyme. Interestingly, this insensitivity does not simultaneously introduce a specificity in the mitochondrial enzyme for G1:U72.

Cocrystal structures solved thus far show that class II enzymes approach the acceptor stem from the major groove side (*65, 66*). In particular, the cocrystal structure of the

class II yeast aspartyl-tRNA synthetase with $tRNA^{Asp}$ showed specific contacts between the enzyme and the 1:72 base pair in the major groove. These contacts involved residues in the flexible loop of motif 2 (*67*).

If the loop of motif 2 in alanyl-tRNA synthetases makes contact with the 1:72 base pair in a manner which is analogous to the aspartyl system, then the cause for the insensitivity of the mitochondrial enzyme to a G1:U72 versus G1:C72 base pair is subtle. Sequence alignment of the two synthetases (Figure 2) revealed that much of the sequence that corresponds to the portion which makes major groove contacts in the aspartyl system is exactly conserved between the two alanine enzymes. Each enzyme has a motif 2 loop of 19 amino acids. In the first 13 residues, the only differences are the replacement of Glu79 and Asn80 in the *E. coli* sequence with a pair of aspartic acid residues. In the C-terminal portion of the loop, the two enzymes are dissimilar, with the exception of a pair of highly conserved histidines (residues 87 and 88 in the *E. coli* sequence). These histidines are shifted by one residue toward the N-terminus in the mitochondrial synthetase. Thus, if the 1:72 base pair interacts with the motif 2 loop of the *E. coli* enzyme, then the removal of these interactions in the mitochondrial enzyme does not involve a deletion but, more likely, a repositioning of the loop.

On the other hand, extensive alanine-scanning mutagenesis of motif 2 of *E. coli* alanyl-tRNA synthetase provided little evidence for important contacts between the tRNA substrate and this region of the protein (*68*). Seryl-tRNA synthetase, another class II synthetase, may provide a better model for interactions between the acceptor stem and the motif 2 loop of the alanyl synthetase. Both the seryl and alanyl synthetases contain motif 2 loops which are long (17 and 19 amino acids, respectively) relative to that of aspartyl-tRNA synthetase (11 residues). In the cocrystal structure of *T. thermophilus* seryl-tRNA synthetase and $tRNA^{Ser}$ (*66*), the loop of motif 2 makes contacts with the phosphate backbone of the acceptor stem nucleotides 69−71, but does not approach the terminus of the helix. It is unknown which residues, if any, make contact with the 1:72 base pair of $tRNA^{Ser}$, because this region of the RNA is disordered in the crystal structure.

On the basis of *in vivo* experiments, McClain et al. (*69*−*71*) suggested that a possible mechanism for substrate recognition by *E. coli* alanyl-tRNA synthetase involved the formation of a distorted RNA conformation in the acceptor stem. This distortion was proposed to be facilitated by the presence of the G3:U70 wobble base pair, which destabilizes the A-form helix of the acceptor stem. [However, recent *in vitro* analyses of duplex and full-length tRNA substrates with mismatches at position 3:70 with the *E. coli* enzyme showed that any contribution of an irregularity to recognition is minor compared to that associated with recognition of specific atomic groups, such as the exocyclic 2-amino group of G3 (*60*).] In a scenario where helical distortion contributes to substrate recognition, there might be a correlation between the helix stability of an RNA substrate and its capacity to be aminoacylated by the alanyl synthetase. Strikingly, our data for the *C. elegans* mitochondrial AlaRS show no such correlation, as the enzyme aminoacylates substrates with large differences in helix stability [a difference in T_m of 37 °C (*vide supra*) between the microhelix based on *E. coli* $tRNA^{Ala}$ and that based on the *C. elegans* mitochondrial tRNA] with virtually identical efficiency. Therefore, at least for the mitochondrial enzyme, helix stability and distortion probably play little or no role in the discrimination of the RNA substrate.

REFERENCES

1. Normanly, J., Ogden, R. C., Horvath, S. J., and Abelson, J. (1986) *Nature 321*, 213−219.
2. Hou, Y. M., and Schimmel, P. (1988) *Nature 133*, 140−145.
3. Normanly, J., and Abelson, J. (1989) *Annu. Rev. Biochem. 58*, 1029−1049.
4. McClain, W. H. (1995) in *tRNA: Structure Function and Biosynthesis* (Söll, D., and RajBhandary, U. L., Eds.) pp 335−347, American Society for Microbiology Press, Washington, DC.
5. Francklyn, C., Musier-Forsyth, K., and Schimmel, P. (1992) *Eur. J. Biochem. 206*, 315−321.
6. Martinis, S. A., and Schimmel, P. (1992) *Proc. Natl. Acad. Sci. U.S.A. 89*, 65−69.
7. Frugier, M., Florentz, C., and Giegé, R. (1992) *Proc. Natl. Acad. Sci. U.S.A. 89*, 3990−3994.
8. Frugier, M., Florentz, C., and Giegé, R. (1994) *EMBO J. 13*, 2218−2226.
9. Hamann, C. S., and Hou, Y.-M. (1995) *Biochemistry 34*, 6527−6532.
10. Quinn, C. L., Tao, N., and Schimmel, P. (1995) *Biochemistry 34*, 12489−12495.
11. Saks, M. E., and Sampson, J. R. (1996) *EMBO J. 15*, 2843−2849.
12. Weiner, A. M., and Maizels, N. (1987) *Proc. Natl. Acad. Sci. U.S.A. 84*, 7383−7387.
13. Maizels, N., and Weiner, A. M. (1994) *Proc. Nat. Acad. Sci. U.S.A. 91*, 6729−6734.
14. Schimmel, P., Giegé, R., Moras, D., and Yokoyama, S. (1993) *Proc. Natl. Acad. Sci. U.S.A. 90*, 8763−8768.
15. Park, S. J., and Schimmel, P. (1988) *J. Biol. Chem. 263*, 16527−16530.
16. Shiba, K., Ripmaster, T., Suzuki, N., Nichols, R., Plotz, P., Noda, T., and Schimmel, P. (1995) *Biochemistry 34*, 10340−10349.
17. Ripmaster, T. L., Shiba, K., and Schimmel, P. (1995) *Proc. Natl. Acad. Sci. U.S.A. 92*, 4932−4936.
18. Rich, A., and RajBhandary, U. L. (1976) *Annu. Rev. Biochem. 45*, 805−860.
19. Crothers, D. M., Seno, T., and Soll, D. G. (1972) *Proc. Natl. Acad. Sci. U.S.A. 69*, 3063−3067.
20. Shi, J.-P., Francklyn, C., Hill, K., and Schimmel, P. (1990) *Biochemistry 29*, 3621−3626.
21. Lee, C. P., Mandal, N., Dyson, M., R., and RajBhandary, U. L. (1993) *Proc. Natl. Acad. Sci. U.S.A. 90*, 7149−7152.
22. Hipps, D., Shiba, K., Henderson, B., and Schimmel, P. (1995) *Proc. Natl. Acad. Sci. U.S.A. 92*, 5550−5552.
23. Sprinzl, M., Horn, C., Brown, M., Ioudovitch, A., and Steinberg, S. (1998) *Nucleic Acids Res. 26*, 148−153.
24. McClain, W. H., and Foss, K. (1988) *Science 241*, 1804−1807.
25. Francklyn, C., and Schimmel, P. (1989) *Nature 337*, 478−481.
26. Shi, J.-P., Martinis, S., and Schimmel, P. (1992) *Biochemistry 31*, 4931−4936.
27. Musier-Forsyth, K., Usman, N., Scaringe, S., Doudna, J., Green, R., and Schimmel, P. (1991) *Science 253*, 784−786.
28. Musier-Forsyth, K., Shi, J.-P., Henderson, B., Bald, R., Fürste, J. P., Erdmann, V. A., and Schimmel, P. (1995) *J. Am. Chem. Soc. 117*, 7253−7254.
29. Shi, J. P., Francklyn, C., Hill, K., and Schimmel, P. (1990) *Biochemistry 29*, 3621−3626.
30. Shi, J.-P., and Schimmel, P. (1991) *J. Biol. Chem. 266*, 2705−2708.
31. Musier-Forsyth, K., and Schimmel, P. (1992) *Nature 357*, 513−515.

32. Beuning, P. J., Gulotta, M., and Musier-Forsyth, K. (1997) *J. Am. Chem. Soc. 119*, 8397−8402.
33. Jasin, M., Regan, L., and Schimmel, P. (1983) *Nature 306*, 441−447.
34. Schimmel, P., and Ripmaster, T. (1995) *Trends Biochem. Sci. 20*, 333−334.
35. Ho, C., Jasin, M., and Schimmel, P. (1985) *Science 229*, 389−393.
36. Buechter, D. D., and Schimmel, P. (1995) *Biochemistry 34*, 6014−6019.
37. Hou, Y.-M., and Schimmel, P. (1989) *Biochemistry 28*, 6800−6804.
38. Wolstenholme, D. R. (1992) *Int. Rev. Cytol. 141*, 173−216.
39. Wolstenholme, D. R., Macfarlane, J. L., Okimoto, R., Clary, D. O., and Wahleithner, J. A. (1987) *Proc. Natl. Acad. Sci. U.S.A. 84*, 1324−1328.
40. Okimoto, R., and Wolstenholme, D. R. (1990) *EMBO J. 9*, 3405−3411.
41. de Bruijn, M. H. L., and Klug, A. (1983) *EMBO J. 2*, 1309−1321.
42. Steinberg, S., Gautheret, D., and Cedergren, R. (1994) *J. Mol. Biol. 236*, 982−989.
43. Barstead, R. J., and Waterson, R. H. (1989) *J. Biol. Chem. 264*, 10177−10185.
44. Studier, F. W., Rosenberg, A. H., Dunn, J. J., and Debendorff, J. W. (1990) *Methods Enzymol. 185*, 60−89.
45. Ribas de Pouplana, L., Buechter, D. D., Davis, M. W., and Schimmel, P. (1993) *Protein Sci. 2*, 2259−2262.
46. Francklyn, C., Musier-Forsyth, K., and Schimmel, P. (1992) *Eur. J. Biochem. 206*, 315−321.
47. Calendar, R., and Berg, P. (1966) *Biochemistry 5*, 1690−1695.
48. Fersht, A. R., Ashford, J. S., Bruton, C. J., Jakes, R., Koch, G. L. E., and Hartley, B. S. (1975) *Biochemistry 14*, 1−4.
49. Eriani, G., Delarue, M., Poch, O., Gangloff, J., and Moras, D. (1990) *Nature 347*, 203−206.
50. Cusack, S., Berthet-Colominas, C., Härtlein, M., Nassar, N., and Leberman, R. (1990) *Nature 347*, 249−255.
51. Wilson, R., Ainscough, R., Anderson, K., Baynes, C., Berks, M., Bonfield, J., Burton, J., Connell, M., Copsey, T., and Cooper, J., et al. (1994) *Nature 368*, 32−38.
52. Solovyev, V. V., Salamov, A. A., and Lawrence, C. B. (1995) in *Third International Conference on Intelligent Systems for Molecular Biology* (Rawling, C. C. D., Altman, R., Hunter, L., Lengauer, T., Wodak, S., Eds.) pp 367−375, AAAI Press, Cambridge, England.
53. Hartl, F. U., and Neupert, W. (1990) *Science 247*, 930−938.
54. Felsenstein, J. (1981) *J. Mol. Evol. 17*, 368−376.
55. Putney, S. D., Sauer, R. T., and Schimmel, P. R. (1981) *J. Biol. Chem. 256*, 198−204.
56. Jasin, M., Regan, L., and Schimmel, P. (1984) *Cell 36*, 1089−1095.
57. Ribas de Pouplana, L., and Schimmel, P. (1997) *Biochemistry 36*, 15041−15048.
58. Regan, L., Bowie, J., and Schimmel, P. (1987) *Science 235*, 1651−1653.
59. Liu, H., Kessler, J., Peterson, R., and Musier-Forsyth, K. (1995) *Biochemistry 34*, 9795−9800.
60. Beuning, P. J., Yang, F., Schimmel, P., and Musier-Forsyth, K. (1997) *Proc. Natl. Acad. Sci. U.S.A. 94*, 10150−10154.
61. Buechter, D. D., and Schimmel, P. (1993) *Biochemistry 32*, 5267−5272.
62. Shiba, K., Schimmel, P., Motegi, H., & Noda, T. (1994) *J. Biol. Chem. 269*, 30049−30055.
63. Chow, C. M., and RajBhandary, U. L. (1993) *J. Biol. Chem. 268*, 12855−12863.
64. Wakasugi, K., Quinn, C. L., Tao, N., and Schimmel, P. (1998) *EMBO J. 17*, 297−305.
65. Cavarelli, J., Rees, B., Ruff, M., Thierry, J.-C., and Moras, D. (1993) *Nature 362*, 181−184.
66. Biou, V., Yaremchuk, A., Tukalo, M., and Cusack, S. (1994) *Science 263*, 1404−1410.
67. Ruff, M., Krishnaswamy, S., Boeglin, M., Poterszman, A., Mitschler, A., Podjarny, A., Rees, B., Thierry, J. C., and Moras, D. (1991) *Science 252*, 1682−1689.
68. Davis, M. W., Buechter, D. D., and Schimmel, P. (1994) *Biochemistry 33*, 9904−9910.
69. McClain, W. H., Chen, Y.-M., Foss, K., and Schneider, J. (1988) *Science 242*, 1681−1684.
70. McClain, W. H., Gabriel, K., and Schneider, J. (1996) *RNA 2*, 105−109.
71. Gabriel, K., Schneider, J., and McClain, W. H. (1996) *Science 271*, 195−197.

BI9804636